Research Article | Vol. 25, No. 26 | 25 Dec 2017 | OPTICS EXPRESS 32757

Optics EXPRESS

Fast-response liquid crystal phase modulators for augmented reality displays

YUGE HUANG, ZIQIAN HE, AND SHIN-TSON WU*

College of Optics and Photonics, University of Central Florida, Orlando, FL 32816, USA
**swu@ucf.edu*

Abstract: We report three new liquid crystal mixtures optimized for the phase modulator of an augmented reality display. The mixtures exhibit a relatively high birefringence (Δn) yet low viscosity, modest dielectric anisotropy (Δε), and acceptable resistivity and UV stability. High Δn enables a thin cell gap (d≈1.7 μm) for achieving 2π phase change with a reflective Liquid-Crystal-on-Silicon (LCoS) device and ~2 ms average phase-to-phase response time at 40°C. The modest Δε helps lower the operation voltage to 5V. To improve the response time of a full-color LCoS, we propose a new driving method by shifting the operation voltage away from the threshold. We also applied such a high Δn LC mixture to LCoS based amplitude modulators and achieved submillisecond response time. Widespread applications of these materials for the emerging augmented reality displays are foreseeable.

OCIS codes: (070.6120) Spatial light modulators; (120.2040) Displays; (160.3710) Liquid crystals.

References and links

1. D. Armitage, I. Underwood, and S.-T. Wu, *Introduction to Microdisplays* (John Wiley & Sons, 2006).
2. A. Maimone, A. Georgiou, and J. S. Kollin, "Holographic near-eye displays for virtual and augmented reality," ACM Trans. Graph. **36**(4), 85 (2017).
3. N. Matsuda, A. Fix, and D. Lanman, "Focal surface displays," ACM Trans. Graph. **36**(4), 86 (2017).
4. P. Sun, S. Chang, S. Zhang, T. Xie, H. Li, S. Liu, C. Wang, X. Tao, and Z. Zheng, "Computer-generated holographic near-eye display system based on LCoS phase only modulator," Proc. SPIE **10396**, 103961J (2017).
5. Y.-W. Li, C.-W. Lin, K.-Y. Chen, K.-H. Fan-Chiang, H.-C. Kuo, and H.-C. Tsai, "Front-lit LCOS for wearable applications," in *SID Int. Symp. Dig. Tech. Pap.* (2014), pp. 234–236.
6. H. Hasebe and S. Kobayashi, "A full-color field sequential LCD using modulated backlight," in *SID Int. Symp. Dig. Tech. Pap.* (1985), pp. 81–83.
7. Y. P. Huang, F. C. Lin, and H. P. D. Shieh, "Eco-displays: The color LCD's without color filters and polarizers," J. Disp. Technol. **7**(12), 630–632 (2011).
8. C. Wang and R. Hsu, "Digital modulation on micro display and spatial light modulator," SID Int. Symp. Dig. Tech. Pap. **48**(1), 238–241 (2017).
9. G. Tan, Y.-H. Lee, F. Gou, H. Chen, Y. Huang, Y.-F. Lan, C.-Y. Tsai, and S.-T. Wu, "Review on polymer-stabilized short-pitch cholesteric liquid crystal displays," J. Phys. D Appl. Phys. **50**(49), 493001 (2017).
10. S. Siemianowski, M. Bremer, E. Plummer, B. Fiebranz, M. Klasen-Memmer, and J. Canisius, "Liquid crystal technologies towards realising a field sequential colour (FSC) display," in *SID Int. Symp. Dig. Tech. Pap.* (2016), pp. 175–178.
11. Y. Huang, H. Chen, G. Tan, H. Tobata, S. Yamamoto, E. Okabe, Y.-F. Lan, C.-Y. Tsai, and S.-T. Wu, "Optimized blue-phase liquid crystal for field-sequential-color displays," Opt. Mater. Express **7**(2), 254–257 (2017).
12. J. Sun and S.-T. Wu, "Recent advances in polymer network liquid crystal spatial light modulators," J. Polym. Sci. Part B Polym. Phys. **52**(3), 183–192 (2014).
13. A. K. Srivastava, V. G. Chigrinov, and H. S. Kwok, "Ferroelectric liquid crystals: Excellent tool for modern displays and photonics," J. Soc. Inf. Disp. **23**(6), 253–272 (2015).
14. H. Chen, F. Gou, and S. T. Wu, "Submillisecond-response nematic liquid crystals for augmented reality displays," Opt. Mater. Express **7**(1), 195–201 (2017).
15. S. Gauza, H. Wang, C.-H. Wen, S.-T. Wu, A. J. Seed, and R. Dabrowski, "High birefringence isothiocyanato tolane liquid crystals," Jpn. J. Appl. Phys. **42**, 3463–3466 (2003).
16. R. Dąbrowski, P. Kula, and J. Herman, "High birefringence liquid crystals," Crystals **3**(3), 443–482 (2013).
17. Y. Chen, J. Sun, H. Xianyu, S.-T. Wu, X. Liang, and H. Tang, "High birefringence fluoro-terphenyls for thin-cell-gap TFT-LCDs," J. Disp. Technol. **7**(9), 478–481 (2011).
18. H. Chen, F. Peng, M. Hu, and S. T. Wu, "Flexoelectric effect and human eye perception on the image flickering of a liquid crystal display," Liq. Cryst. **42**(12), 1730–1737 (2015).

#310220 https://doi.org/10.1364/OE.25.032757
Journal © 2017 Received 30 Oct 2017; revised 7 Dec 2017; accepted 11 Dec 2017; published 15 Dec 2017

Optics EXPRESS

19. S.-T. Wu, U. Efron, and L. D. Hess, "Birefringence measurements of liquid crystals," Appl. Opt. **23**(21), 3911–3915 (1984).
20. I. Haller, "Thermodynamic and static properties of liquid crystals," Prog. Solid State Chem. **10**(2), 103–118 (1975).
21. K. Beeson, S. Zimmerman, W. Livesay, R. Ross, C. Livesay, and K. Livesay, "LED-based light-recycling light sources for projection displays," in *SID Int. Symp. Dig. Tech. Pap.* (2006), pp. 1823–1826.
22. S.-T. Wu, "Birefringence dispersions of liquid crystals," Phys. Rev. A Gen. Phys. **33**(2), 1270–1274 (1986).
23. S.-T. Wu and C.-S. Wu, "Rotational viscosity of nematic liquid crystals A critical examination of existing models," Liq. Cryst. **8**(2), 171–182 (1990).
24. C.-H. Wen, S. Gauza, and S.-T. Wu, "Photostability of liquid crystals and alignment layers," J. Soc. Inf. Disp. **13**(9), 805–811 (2005).
25. J. Sun, Y. Chen, and S.-T. Wu, "Submillisecond-response and scattering-free infrared liquid crystal phase modulators," Opt. Express **20**(18), 20124–20129 (2012).
26. S.-T. Wu, "Design of a liquid crystal based tunable electrooptic filter," Appl. Opt. **28**(1), 48–52 (1989).
27. S.-T. Wu and C.-S. Wu, "Mixed-mode twisted nematic liquid crystal cells for reflective displays," Appl. Phys. Lett. **68**(11), 1455–1457 (1996).

1. Introduction

Liquid-Crystal-on-Silicon (LCoS) panels have found promising applications in augmented reality (AR) near-eye displays because of their low operation voltage, high resolution density, broad bandwidth, compact size, and light weight [1–5]. Both amplitude modulation and phase modulation using LCoS have been demonstrated: 1) For amplitude modulation, 1π phase retardation and high contrast ratio are critically needed, making reflective 90° mixed-mode twist nematic (MTN) and vertical alignment (VA) LCoS panels two favored choices. Most commercially available AR devices are based on MTN LCoS panels, such as Google Glass and Microsoft HoloLens. 2) Phase modulation requires a minimum 2π-phase change. Because the information encoded in an amplitude modulator is limited, to generate high-quality 3D images in AR displays, phase-only LCoS is receiving increasing attention. In 2017, Microsoft demonstrated an AR prototype using a phase-only holographic projection [2], and Oculus proposed a novel focal surface display with a phase-only LCoS [3]. In these prototypes, field-sequential-color (FSC) display technology [6] was applied to mitigate the noticeable screen door effect due to inadequate resolution density. Although FSC operation triples the pixel density, the refresh rate also needs to be tripled to eliminate unwanted color breakup [7]. Presently, Both Microsoft and Oculus devices were operated at 60 Hz, which is 4x slower than the desired 240 Hz. The challenge for enabling a high refresh rate depends on the driving scheme. For digital driving, a maximum voltage, say V_{max} ~6 V, is applied and the grayscale is controlled by the pulse width modulation technique [8]. Digital driving offers good grayscale accuracy and fast response time for amplitude modulators, but for phase modulation it suffers from digital flicker noise the high power consumption. The incurred digital flicker noise results from transient LC reorientation between pulses, which in turn generates an unstable wavefront. By contrast, in analog driving, a constant voltage is applied to the whole frame. As a result, the LC can keep its orientation steadily and the resultant phase is stable. The major drawback of analog driving is its slower response time, especially when the gray level is near the threshold voltage. For 240-Hz operation, the LC response time should be less than 4 ms. To mitigate color breakup, submillisecond response time is highly desirable.

To achieve fast response time, several approaches have been investigated, such as polymer-stabilized short-pitch cholesteric LCs [9–11], polymer network LCs [12], and ferroelectric LCs [13]. The former two approaches indeed offer submillisecond response time, but the required voltage is quite high, which exceeds the sustainable voltage (6 V) of LCoS backplanes. Ferroelectric LC is bi-stable, and is difficult to provide continuous phase gray scale, unless multi-domain structure or digital driving method are utilized. In general, nematic LC has a relatively slow response time (5-10 ms). Recently, a submillisecond–response nematic LC mixture for VA LCoS intensity modulator has been reported [14]. However, to achieve 2π phase change, the required cell gap is twice thicker than that of a corresponding intensity modulator, which in turn leads to a 4x slower response time. High birefringence LC

Optics EXPRESS

materials enable a thin cell gap to achieve fast response time. Several high birefringence (Δn>0.25) LC compounds have been developed, such as NCS-tolane [15,16] and terphenyls [17]. Each compound has its own unique properties. For examples, tolane has high Δn and low viscosity, but its UV stability is a concern. On the other hand, terphenyl has high Δn and good UV stability, but its melting temperature is relatively high. There is an urgent need to develop high Δn LC mixtures with low viscosity, reasonably high resistivity (>10^{12} Ω·cm), wide nematic range, and modest dielectric anisotropy for fast-response phase modulator applications.

In this paper, we report three nematic LC mixtures optimized for phase-only LCoS. Their high birefringence (Δn~0.25 at T = 25°C and λ = 550 nm) and low rotational viscosity (γ_1~130 mPa·s) jointly contribute to a fast response time (2.08 ms), which enables 240 Hz refresh rate without the annoying image flickering [18]. Their relatively large dielectric anisotropy ($\Delta\varepsilon$> 6.6) helps to lower the operation voltage to about 5 V. When used in a reflective 90° MTN cell for amplitude modulation, submillisecond response time (0.90 ms) and high contrast ratio (2097:1) are achieved at 5 V, which enables 1 kHz frame rate operation.

2. Material characterization

We use LC-1, LC-2 and LC-3 to denote the three new LC mixtures, developed by DIC Corporation. Their physical properties were characterized at temperature T = 25°C and results are summarized in Table 1. We measured the melting temperature (T_m) and clearing temperature (T_c) by Differential Scanning Calorimetry (DSC, TA instruments Q100). The wide nematic range (<-35°C ~85°C) satisfies the requirement for most AR applications. We also measured the dielectric constants with a multi-frequency LCR meter HP-4274. The reasonably large $\Delta\varepsilon$ contributes to a low operation voltage, which is desirable for head-mounted display devices. The rotational viscosity γ_1 and [splay, twist, bend] elastic constants [K_{11}, K_{22}, K_{33}] were measured through transient current method by autronic-MELCHRS LCCS107. The low viscosity (γ_1~130 mPa·s) helps reduce the response time effectively. For active matrix displays, the LC resistivity should be higher than 10^{13} Ω·cm, while for LCoS it can be reduced to 10^{12} Ω·cm because of the higher frame rate. The resistivity of our three LC mixtures satisfies this requirement.

Table 1. Measured physical properties of LC-1, LC-2, and LC-3 at T = 25°C.

LC mixture	LC-1	LC-2	LC-3
T_c (°C)	86.5	84.9	85.7
T_m (°C)	< –40	–35.4	< –40
Δn @550 nm	0.251	0.247	0.25
$\Delta\varepsilon$ @1 kHz	6.68	9.1	6.75
$\varepsilon_{\perp}$ @1 kHz	3.5	3.83	3.41
γ_1 (mPa·s)	133	130	123
K_{11} (pN)	12.1	11.7	12.2
K_{22} (pN)	7.6	6.8	7.4
K_{33} (pN)	15.4	14.4	14.6
γ_1/K_{11} (ms/μm^2)	11.0	11.1	10.1
Resistivity (Ω·cm)	1.6×10^{12}	7.0×10^{11}	8.8×10^{11}

Optics EXPRESS

2.1 Birefringence

Birefringence determines the cell gap, which in turn affects the response time. To measure Δn, we filled each LC mixture into a homogeneous cell with cell gap d = 5 μm. The pretilt angle of the rubbed polyimide alignment layers is about 3°. We sandwiched each cell between crossed polarizers and activated it with a 1-kHz square-wave AC voltage. The birefringence was calculated from the measured phase retardation [19]. Figure 1(a) depicts the temperature-dependent birefringence at λ = 632.8 nm (He-Ne laser). The sample temperature was controlled by a Linkam heating stage through a temperature programmer TMS94. The extrapolated birefringence Δn_0 at T = 0K and the exponent β were obtained by fitting experimental data with Eq. (1) [20] and results are listed in Table 2.

$$\Delta n = \Delta n_0 S = \Delta n_0 \left(1 - T / T_c\right)^{\beta}. \tag{1}$$

For a working LCoS device, its operating temperature is about 40°C due to the thermal effects of backplane and the light source [21]. Therefore, we focus our studies at 40°C. To measure the wavelength dispersion, in experiment we used a He-Ne laser (λ = 632.8 nm) and a tunable Argon ion laser (λ = 457 nm, 488 nm and 514 nm). Results are plotted in Fig. 1(b). The single-band birefringence dispersion equation [22] was used for fitting:

$$\Delta n = G \frac{\lambda^2 \lambda^{*2}}{\lambda^2 - \lambda^{*2}}, \tag{2}$$

where G is a proportionality constant and λ* is the mean resonance wavelength. At λ = 633 nm and 40°C, the Δn of [LC-1, LC-2, LC-3] is [0.2233, 0.2213, 0.2207], respectively. The obtained G & λ* values are also listed in Table 2.

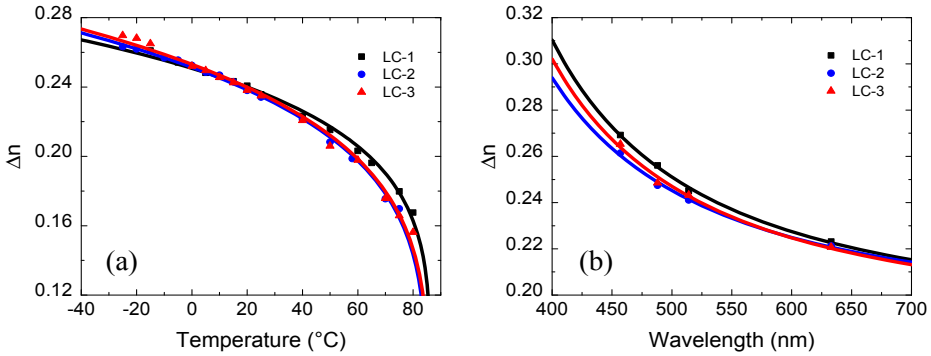

Fig. 1. (a) Temperature-dependent birefringence at λ = 633 nm, 1 kHz. (b) Dispersion of birefringence at 1 kHz, 40°C. Dots are measured data; lines in (a) and (b) are fitting curves with Eq. (1) and Eq. (2), respectively.

Table 2. Fitting parameters obtained through Eqs. (1)-(3).

LC mixture	Δn_0	β	G @40°C (μm^{-2})	λ* @40°C (μm)	A (ms/μm^2)	E_a (meV)
LC-1	0.318	0.167	2.96	0.251	3.00×10^5	315.8
LC-2	0.334	0.197	3.32	0.239	5.36×10^6	355.1
LC-3	0.338	0.202	3.05	0.247	1.80×10^6	377.4

2.2 Visco-elastic coefficient

We also measured the transient decay curves of these LC mixtures and obtained the temperature-dependent visco-elastic coefficient γ_1/K_{11}, as the dots presented in Fig. 2. The solid lines represent fittings with following relation [23]:

Optics EXPRESS

$$\frac{\gamma_1}{K_{11}} = A\frac{\exp\left(E_a / k_B T\right)}{\left(1 - T / T_c\right)^{\beta}}. \tag{3}$$

Here, A, E_a, and k_B stand for the proportionality constant, Boltzmann constant, and activation energy, respectively. The fitting parameters are also included in Table 2. From Fig. 2 and Eq. (3), we can see that γ_1/K_{11} decreases dramatically as the temperature increases. At 40°C, the γ_1/K_{11} of [LC-1, LC-2, LC-3] is [5.8, 6.0, 5.15] ms/μm^2, respectively.

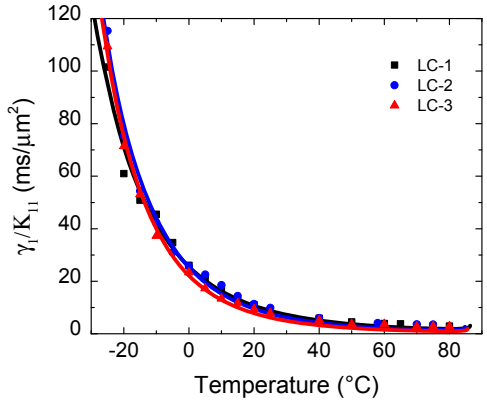

Fig. 2. Temperature-dependent visco-elastic coefficient at λ = 633 nm and 1 kHz. Dots are measured data and lines are fitting curves with Eq. (3).

2.3 Photostability

During the fabrication process, an LCoS panel is usually exposed to UV light in order to seal the filling hole. Such a UV exposure could damage the LC mixture or the alignment layer, depending on the photostability of employed LC and alignment materials. If an LCoS is using a low birefringence LC and inorganic alignment layers, such as silicon-dioxide (SiO_2), then the photostability is not a concern [24]. However, to increase birefringence while keeping a low viscosity, a small percentage (5-10 wt.%) of tolane compounds is often added to the mixtures, which is sensitive to UV light.

To investigate photostability, we chose LC-1 as an example for this study because it has the widest nematic range and highest resistivity among the three samples listed in Table 1. In experiment, we injected LC-1 into two 9.3-μm-thick homogeneous cells with SiO_2 alignment layers. We measured the birefringence and visco-elastic coefficient of the samples after UV exposure and recorded the changes in Fig. 3. Figure 3(a) depicts the measured photo-stability of LC-1 at λ = 365 nm. As the UV dosage increases, Δn decreases and γ_1/K_{11} increases slightly. Compared to the initial value, Δn decreases 4.1% whereas γ_1/K_{11} increases 4.3% after 20 J/cm^2 of UV exposure and then saturates. In LCD industry, to seal the LC filling hole, a λ = 365 nm UV light with dosage of ~10 J/cm^2 is commonly used. This indicates that LC-1 is relatively UV-robust, considering its high birefringence and low visco-elastic constant. However, to prevent photo-degradation, we still recommend blocking the LC area during UV exposure. An alternative choice is to use a longer wavelength UV, say λ = 385 nm [25]. From the measured photo-stability results in Fig. 3(b), even after 120 J/cm^2 of UV exposure at λ = 385 nm, its Δn only drops by 3.1% as compared to the initial value, while γ_1/K_{11} fluctuates within 1.6% variation.

Optics EXPRESS

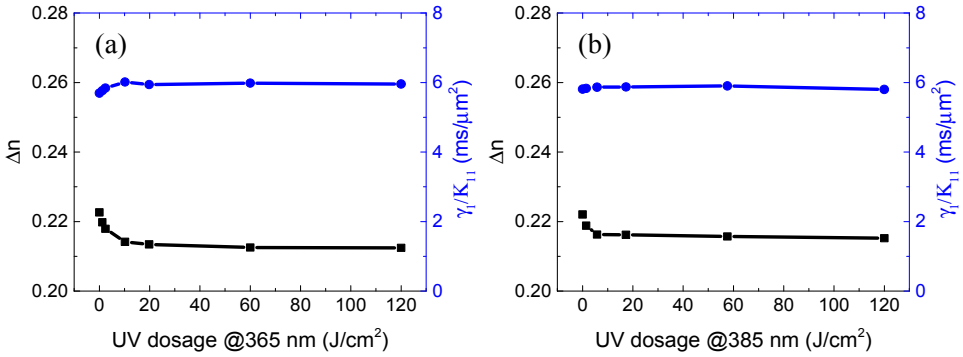

Fig. 3. Measured photo-stability of LC-1 with an UV LED at (a) 365nm and (b) 385nm. Probing laser beam: λ = 633 nm. Measurement temperature: 40°C. Black rectangles denote birefringence and blue circles denote visco-elastic constant.

3. 2π phase modulation in homogeneous-aligned cells

3.1 Voltage-dependent phase change (V-Φ) curves

To simulate the performance in a real LCoS device, we filled each LC mixture into a transmissive homogeneous cell with cell gap d≈3.4 μm. This is the thinnest cell gap we have in our labs. Its phase retardation is equivalent to that of a reflective 1.7-μm-thick cell, because of the doubled optical path. Using the physical parameters measured at λ = 633 nm and 40°C, we simulated the voltage-dependent transmittance (VT) curves by a commercial LCD simulator DIMOS 2.0. Figure 4 compares the V-Φ curves converted from the measured VT curves (dots) and the simulated VT curves (lines). The simulation agrees well with experiment.

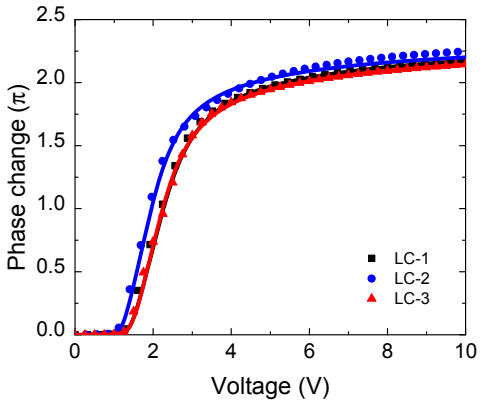

Fig. 4. Measured and simulated V-Φ curves at 40°C, λ = 633 nm and 1 kHz. Dots are measured data in transmissive homogenous cells with d~3.4 μm; lines are simulated curves in reflective homogenous cells with d~1.7 μm.

3.2 Response time

The response time (τ) of an LC cell is proportional to d^2. Thus, the response time of our 3.4-μm transmissive cell is expected to be 4x longer than that of a 1.7-μm-thick reflective cell. Table 3 compares the measured and simulated response times. For each LC mixture, the first row represents the measured result of the transmissive cell; the second row is the extrapolated result for the reflective LCoS, where the cell gap is half and the response time is one-fourth of the transmissive cell, and the third row is the simulated result of a reflective cell. Good agreement is achieved between experiment and simulation.

Optics EXPRESS

Table 3. Response time of measured, extrapolated and simulated results at 40°C, λ = 633 nm and 1 kHz.

LC mixture	Type		d (μm)	$V_{2\pi}$ (V)	τ_{on} (ms)	τ_{off} (ms)	$\tau_{on} + \tau_{off}$ (ms)
LC-1	Measured	Transmissive	3.40	5.38	1.23	7.82	9.05
	Extrapolated	Reflective	1.70	5.38	0.31	1.95	2.26
	Simulated		1.66	5.38	0.37	2.21	2.58
LC-2	Measured	Transmissive	3.44	4.57	1.44	8.15	9.59
	Extrapolated	Reflective	1.72	4.57	0.36	2.04	2.40
	Simulated		1.67	4.57	0.40	2.34	2.74
LC-3	Measured	Transmissive	3.39	5.78	0.96	6.65	7.61
	Extrapolated	Reflective	1.69	5.78	0.24	1.66	1.90
	Simulated		1.65	5.78	0.28	2.00	2.28

Table 4. Selected nine phase levels between 0 and 2π, and the corresponding operation voltage of LC-1. The listed data are obtained from Fig. 4.

Phase level	1	2	3	4	5	6	7	8	9
Phase change (π)	0	0.25	0.5	0.75	1	1.25	1.5	1.75	2
Voltage (V)	0	1.52	1.72	1.95	2.21	2.46	2.77	3.42	5.38

Table 5. Measured PTP response time of LC-1 in a transmissive homogenous cell with d = 3.4 μm. Note: the LCoS response time with d = 1.7 μm is 4x faster than the data shown here.

	Rise time (ms)								
Decay time (ms)	1	2	3	4	5	6	7	8	9
1	*	44.47	25.83	17.02	12.29	9.16	6.78	3.55	1.23
2	8.27	*	17.34	13.07	10.06	7.77	5.56	3.01	1.03
3	7.75	21.36	*	11.76	9.12	6.81	4.60	2.58	0.91
4	7.82	20.31	14.40	*	8.07	6.05	3.61	2.32	0.82
5	7.64	17.77	13.57	9.18	*	5.52	3.39	2.15	0.79
6	7.57	13.97	11.95	8.51	6.68	*	3.35	2.04	0.78
7	7.56	14.90	10.89	7.82	6.29	4.37	*	2.10	0.80
8	7.57	15.24	10.39	7.73	6.33	4.89	4.04	*	0.77
9	7.82	14.88	10.15	7.83	6.56	4.76	3.92	2.10	*

In an AR device, the LCoS panel is expected to tune the phase change continuously from 0 to 2π. Here, we selected nine phase levels to represent the full phase tuning range. By measuring the response time between two levels, we can obtain a phase-to-phase (PTP) response time chart. Still using LC-1 as the example, Table 4 lists the representative phase levels and the corresponding operation voltage of the 3.4-μm-thick homogenous cell, while Table 5 summarizes the measured PTP response time without overdrive/undershoot circuitry. The measured average PTP response time is 8.32 ms. Therefore, for $V_{2\pi}$ = 5.38 V, the extrapolated PTP response time for a reflective LCoS panel is 2.08 ms, which enables 240-Hz refresh rate.

3.3 New driving method on a full-color phase-only SLM device

After validating the reliability of our simulation, we simulated the V-Φ curves of LC-1 for RGB colors. From Fig. 1(b) and Eq. (2), the Δn at 40°C and λ = [448 nm, 524 nm, 638 nm] are [0.2739, 0.2437, 0.2220]. These values are the wavelengths of three laser diodes employed in Microsoft's LCoS-based AR prototypes [2]. Either for color filter-type or for FSC-type LCoS [6], the cell gap for RGB colors should be the same since only one panel is utilized. In simulation, the cell gap was set at 1.716 μm to ensure $V_{2\pi} \leq 5$ V works for all three colors. As demonstrated in Fig. 5, the red color with the longest λ and the lowest Δn has the highest $V_{2\pi}$ = 5 V. For green and blue colors, more than 2π phase change can be obtained within 5 V. Thus, we can choose a preferred 2π phase range to use for the green and blue colors. Here we denote V_1 and V_2 as the initial and final voltage of the selected 2π phase

Optics EXPRESS

range. Here, V_2 is higher than V_{th} (threshold voltage), but V_1 can be higher or lower than V_{th}. Under such condition, The LC rise time and decay time depend on the V_1 and V_2 as follows [26]:

$$\tau_{on} = \frac{\tau_0}{(V_2 / V_{th})^2 - 1}, \tag{4a}$$

$$\tau_{off} = \frac{\tau_0}{\left|(V_1 / V_{th})^2 - 1\right|}, \tag{4b}$$

where τ_0 ($= \gamma_1 d^2 / K_{11}\pi^2$) is the free relaxation time, i.e. $V_1 = 0$. From Eq. (4), the response time near V_{th} is slow. If we set $V_1 = 0$ for the blue wavelength, then its V_2 could be not too far from V_{th}, resulting in a slow response time, as Table 6 shows.

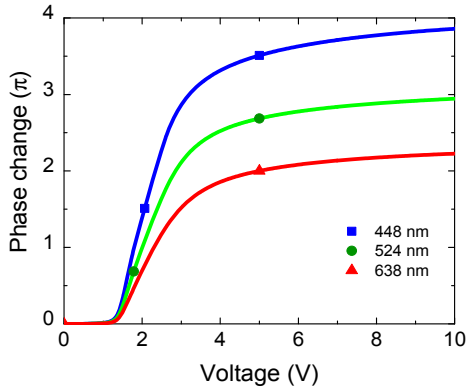

Fig. 5. Simulated V-Φ curves of LC-1 for RGB colors at 40°C in a reflective homogenous cell with d = 1.716 μm. Lines are V-Φ curves; dots mark the lower and upper limit of the 2π phase change range with V_2 = 5 V.

To overcome the above problem, we propose a new driving method to accelerate the response time of an LCoS panel intended for full-color operation. As demonstrated in Table 6, we manually set the same V_2 for all of the RGB colors, say V_2 = 5 V. The dots in Fig. 5 mark the V_1 and V_2 in this design. For green and blue colors, $V_1 > V_{th}$ is achieved. The simulated $\tau_{on} + \tau_{off}$ in Table 6 shows the improvement over the driving method starting from $V_1 = 0$.

Table 6. Simulated response time of LC-1 at 40°C in a reflective homogenous cell with d = 1.716 μm.

λ (nm)	Δn	V_1 (V)	V_2 (V)	τ_{on} (ms)	τ_{off} (ms)	$\tau_{on} + \tau_{off}$ (ms)
448	0.2739	(0.00)	2.34	3.62	2.41	6.03)
		2.07	5.00	0.34	2.76	3.10
524	0.2437	(0.00)	2.86	2.18	2.45	4.63)
		1.78	5.00	0.38	3.43	3.81
638	0.2220	0.00	5.00	0.51	2.48	2.99

A more dramatic improvement can be found in PTP response time because we intentionally shift V_1 and V_2 away from V_{th}. The slow PTP response time in the vicinities of V_{th} is replaced by the fast-response components at high voltage. Tables 4 and 5 illustrate this concept. Here, V_{th} = 1.34 V is between phase level 1 and phase level 2. To get 1π phase change, we can either choose phase levels 1-5 or phase levels 5-9. Covering V_{th}, the average PTP response time between phase levels 1-5, the average value in the left top rectangle in Table 5, is as slow as 14.86 ms. While for phase levels 5-9 above V_{th} (the right bottom rectangle in Table 5), the average value is 3.58 ms, which is more than 4x faster than that of

Optics EXPRESS

phase levels 1-5. For homogeneous-aligned cells, the average PTP response time is comparable with the sum of rise time and decay time. Table 5 confirms this phenomenon, where the average PTP response time 8.32 ms is comparable with $\tau_{on} + \tau_{off} = 9.05$ ms. Using our new driving method, the response time ($\tau_{on} + \tau_{off}$) of all three primary colors is less than 4 ms, indicating <4 ms average PTP response time for RGB colors. This enables 240-Hz operation though a few slow-response phase levels are compromised.

4. Amplitude modulation with a 90° MTN cell

4.1 Voltage-dependent transmittance (V-T) curve

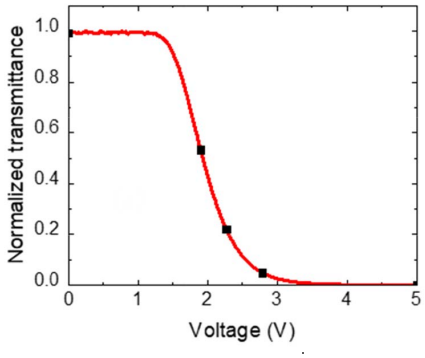

Fig. 6. Measured VT curve in a reflective 90° MTN cell with d = 1.32 μm at 40°C, λ = 633 nm and 1 kHz. Dots mark the gray levels in Table 7.

To explore the performance of our new LC mixtures in projection displays, we fabricated a 90° MTN cell and filled LC-1 into it. A mirror was placed behind the cell to generate reflective mode. A polarizing beam splitter (PBS) was employed functioning as two crossed polarizers. Again, we measured the V-T curve at 40°C, λ = 633 nm and 1 kHz frequency. As depicted in Fig. 6, the measured contrast ratio is 2097:1 at 5 V. The cell gap of the fabricated reflective 90° MTN cell was d = 1.32 μm, which is acceptable for mass production. If we control $d\Delta n$~240 nm, then the peak transmittance should be 88% [27].

4.2 Response time

Due to the employed thin cell gap, sub-millisecond response time was achieved on this MTN cell. At 5 V, the [rise, decay] time is [0.136, 0.698] ms. The measured gray-to-gray (GTG) response time is summarized in Table 7. The gray level (GL, 0-255) was calculated from transmittance (T) by $T = (GL/255)^{2.2}$. The submillisecond average GTG response time (0.90 ms) without overdrive and undershoot circuitries enables 1 kHz frame rate operation, which helps reduce color breakup in FSC displays.

Table 7. Measured GTG response time of LC-1 in a 90° MTN cell with d = 1.32 μm.

	Rise time (ms)					
Decay time (ms)	**GL**	**255**	**192**	**128**	**64**	**0**
	255	*	2.401	1.363	0.648	0.136
	192	0.781	*	1.339	0.517	0.110
	128	0.762	1.916	*	0.493	0.123
	64	0.731	1.743	1.078	*	0.260
	0	0.698	1.619	0.825	0.476	*

5. Conclusion

We have developed three practical LC mixtures for phase-only LCoS-based augmented reality displays. The mixtures exhibit a high birefringence to enable thin cell gap for 240-Hz

Optics EXPRESS

refresh rate, modest dielectric anisotropy for 5V operation voltage, acceptable resistivity and UV stability, and wide nematic range. We also proposed a new driving scheme to improve the response time of a full-color phase-only LCoS panel. When these mixtures are used in MTN LCoS amplitude modulators, submillisecond response time was achieved, enabling 1 KHz operation. Widespread applications of these mixtures for the emerging augmented reality displays are foreseeable.

Funding

Air Force Office of Scientific Research (AFOSR) (FA9550-14-1-0279).

Acknowledgments

We are indebted to DIC Corporation for providing the LC samples, Dr. Simon Fan-Chiang of Himax Display, Engle Liao and Dr. Haiwei Chen, Fangwang Gou, Md Javed Rouf Talukder and Yun-Han Lee for helpful discussion and technical support.